

Article

Supramolecular Catalysis with Chiral Mono- and Bis-(Thio)Urea-Derivatives

Veronica Iuliano , Paolo Della Sala , Carmen Talotta , Margherita De Rosa , Carmine Gaeta ,
Placido Neri * and Annunziata Soriente *

Dipartimento di Chimica e Biologia “A. Zambelli”, Università di Salerno, Via Giovanni Paolo II, Fisciano, I-84084 Salerno, Italy; viuliano@unisa.it (V.I.); pdellasala@unisa.it (P.D.S.); ctalotta@unisa.it (C.T.); maderosa@unisa.it (M.D.R.); cgaeta@unisa.it (C.G.)

* Correspondence: neri@unisa.it (P.N.); titti@unisa.it (A.S.)

Abstract: Chiral mono- and bis-(thio)urea supramolecular organocatalysts were studied in the enantioselective vinylogous addition reaction of 2-trimethylsilyloxyfuran (TMSOF) to carbonylic compounds; the corresponding chiral γ -hydroxymethyl-butenolides are obtained in good yields and with high enantiomeric excesses. The catalyst structure, as well as the reaction conditions, strongly influence the efficiency of the reaction. The conformational features of mono(thio)urea catalysts **2** and **3** and bis(thio)urea catalysts **7** and **8** were investigated by DFT calculations along with the structure of their complexes with benzaldehyde. Natural Bond Orbital (NBO) and Non-Covalent Interaction (NCI) calculations provided useful information concerning the activating H-bonding interactions in the complexes.

Keywords: (thio)ureas; enantioselective synthesis; supramolecular organocatalysis; aldehyde addition; 2-trimethyl-silyloxyfuran; NBO and NCI calculations



Citation: Iuliano, V.; Della Sala, P.; Talotta, C.; De Rosa, M.; Gaeta, C.; Neri, P.; Soriente, A. Supramolecular Catalysis with Chiral Mono- and Bis-(Thio)Urea-Derivatives. *Organics* **2024**, *5*, 32–45. <https://doi.org/10.3390/org5020003>

Academic Editor: Michal Szostak

Received: 29 June 2023

Revised: 2 August 2023

Accepted: 11 March 2024

Published: 26 March 2024



Copyright: © 2024 by the authors. Licensee MDPI, Basel, Switzerland. This article is an open access article distributed under the terms and conditions of the Creative Commons Attribution (CC BY) license (<https://creativecommons.org/licenses/by/4.0/>).

1. Introduction

In “Artificial Enzymes” published in 1982, Breslow [1] envisioned that simple catalysts constituted by small organic molecules can reach performances of natural systems such as selectivity, efficiency, geometric control, and velocity. Since then, very important results have been obtained in the field of supramolecular organocatalysis [2–14] thanks to the design of catalysts inspired by the efficiency of natural enzymes. In supramolecular organocatalysis, different substrate activation modes have been reported [3–14] including iminium catalysis, enamine catalysis, and acid–base organocatalysis [2]. In this context, substrate activation by secondary interactions, such as H-bonding interactions, has played a crucial role in the development of the field [15–17]. Thus, a plethora of organocatalysts embedded with functions able to establish H-bonding interactions have been reported and, among them, urea and thiourea groups have been particularly investigated. Both ureas and thioureas, which have shown a dual behavior acting as both H-bond donor and acceptor, have also been employed in a variety of diastereo- and/or enantioselective processes [15,18]. Regarding different H-bonding supramolecular organocatalysts, in 2008, some of us [19] reported that a calixpyrrole acts as an effective H-bonding donor organocatalyst for the hetero-Diels–Alder reaction of Danishefsky’s diene with aromatic aldehydes. Interestingly, calix[4]pyrrole derivatives showed organocatalytic activities in the diastereoselective vinylogous addition reaction of 2-trimethylsilyloxyfuran (TMSOF) to aldehydes [20].

During our studies focusing on the development of efficient organocatalysts (**1–3**) (Figure 1a) for the addition reaction of 2-trimethylsilyloxyfuran **4** to aldehydes [21], we found that the urea catalyst **1** activated the carbonyl compounds by H-bonding interactions and accelerated the vinylogous aldol reaction (Figure 1b).

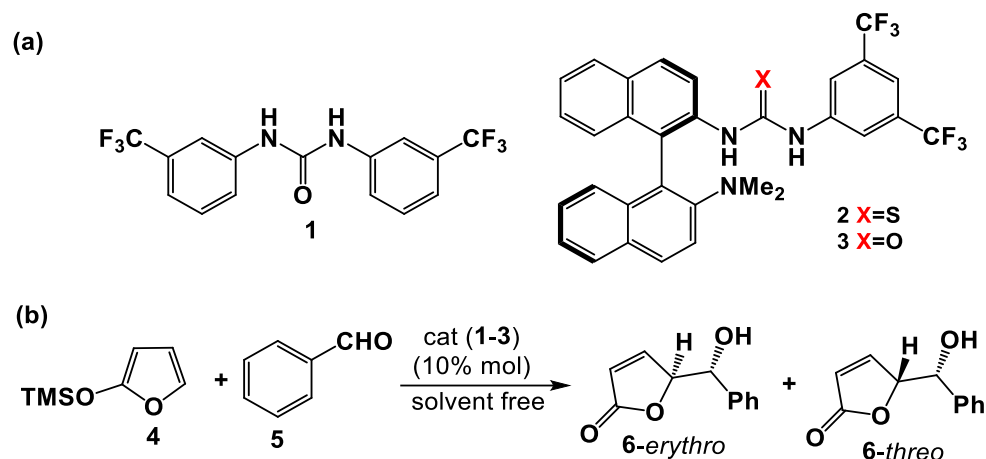
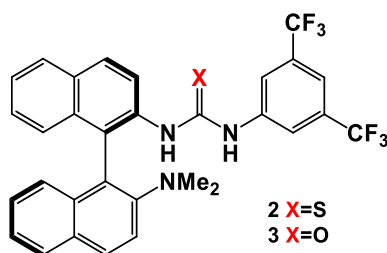


Figure 1. (a) Organocatalysts 1–3; (b) vinyllogous aldol reaction catalyzed by urea 1.

The products of this versatile carbon–carbon bond forming reaction contain a γ -butenolide ring, which represents a substructure of more complex moieties in numerous biologically important natural and synthetic products [22–26]. Several papers describe the diastereoselective addition of variously substituted furan-based silyloxy diene synthons to a variety of achiral aldehydes and acetals using Lewis acids as catalysts [27,28], and MacMillan [29] reported the first enantioselective organocatalytic 1,4-addition of TMSOF to unsaturated aldehydes with high enantioselectivities [30,31].

Herein, we report a detailed study on the reactivity of chiral (thio)urea-derivatives 2/3 and 7/8 in the vinyllogous aldol reaction of TMSOF 4 to carbonylic compounds that afford chiral hydroxy-butenolides 6 in good yields and high enantioselectivity (Tables 1 and 2). A detailed computational investigation has been performed to study the conformational features of organocatalysts and their complexes with aldehydes. The experimental trend of catalytic activity is well explained by H-bonding features in the organocatalyst/aldehyde complexes.

Table 1. Addition reaction of TMSOF 4 to benzaldehyde 5 catalyzed by bis(thio)urea catalysts 2 and 3¹.



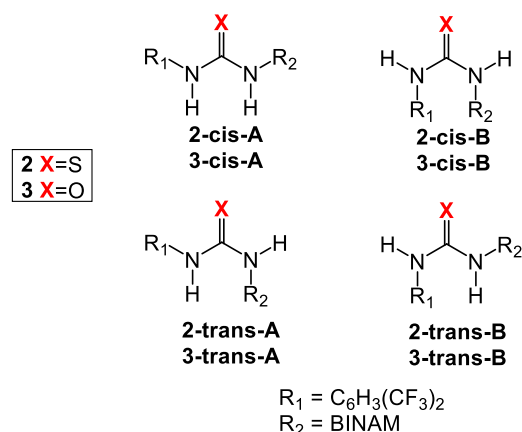
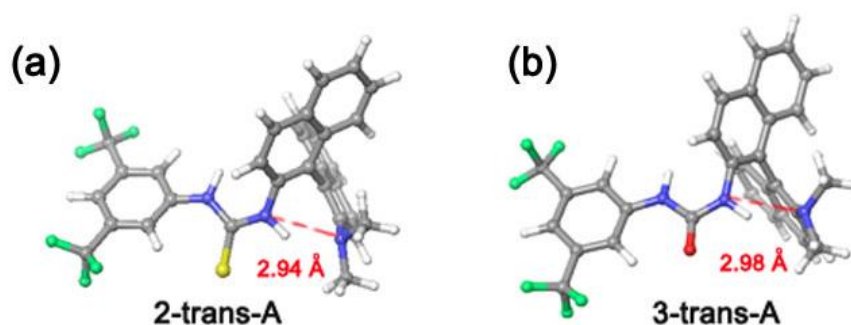
Entry	Catalyst	Equivalents of Aldehyde	T/t (°C/h)	Yield (%) ²	d.r. Erythro/Threo ³	e.e. ⁴ Erythro (%)	e.e. ⁴ Threo (%)
1	2	5	Rt/24	29	70/30	9	21
2	3	5	Rt/24	56	70/30	20	26

¹ The reactions were performed with 0.5 mmol of TMSOF and 10 mol% catalyst was used. ² Isolated yield. ³ The diastereoisomeric ratio was calculated by ¹H NMR of the crude product according to the literature data [31]. ⁴ The e.e. values were determined by chiral HPLC analysis.

Table 2. Relative stabilities between rotamers of Figure 2 and coordination energies of a benzaldehyde molecule 5 to 2-*cis/trans*-A and 3-*cis/trans*-A (Figure 3a,b) catalysts.

Rotamers	$\Delta E_{\text{isomer}}^1$ (kcal/mol)	E_{coord} (kcal/mol)	Yield (%)
2- <i>trans</i> -A	0.0	-	-
2- <i>trans</i> -B	3.0	-	-
2- <i>cis</i> -A	2.1	-	-
2- <i>cis</i> -B	2.5	-	-
3- <i>trans</i> -A	0.0	-	-
3- <i>trans</i> -B	3.4	-	-
3- <i>cis</i> -A	0.7	-	-
3- <i>cis</i> -B	8.9	-	-
5@2- <i>cis</i> -A	1.5	-5.4	29
5@2- <i>trans</i> -A	0.0	-4.7	-
5@3- <i>cis</i> -A	0.0	-7.8	56
5@3- <i>trans</i> -A	1.4	-5.7	-

¹ ΔE_{isomer} is calculated assuming the energy of the most stable conformer as zero.

**Figure 2.** Possible rotamers of derivatives 2 and 3.**Figure 3.** DFT-optimized structures of the most stable rotamer of organocatalysts 2 (a) and 3 (b). N-H...N distances are also reported.

2. Materials and Methods

2.1. General Remarks

All the solvents were reagent grade, and they were dried and freshly distilled before use. Unless specifically mentioned, all reactions were carried out under an argon atmosphere. Purifications of the products were performed by column chromatography (silica gel, Merck, Darmstadt, Germany). Starting materials and all the other reagents were purchased from Aldrich and used without further purification. The NMR spectra (Bruker DRX 400 (^1H 400 MHz; ^{13}C 100 MHz)), were performed in CDCl_3 solution and referenced to residual CHCl_3 (7.26 ppm (^1H); 77.23 ppm (^{13}C)). Chemical shifts are reported in ppm,

multiplicities are indicated by s (singlet), d (doublet), dd (double doublet), t (triplet), dt (double triplet), q (quartet), m (multiplet), and brs (broad singlet). Coupling constants (J) are reported in Hz. Compounds **2** [32,33], **7** [34], and **8** [34] were synthesized according to the literature procedures. Product **6** obtained was compared with the literature [35].

(*R*)-1-[3,5-Bis(trifluoromethyl)phenyl]-3-[1-(2-(dimethylamino)naphthalen-1-yl)naphthalen-2-yl] urea (**3**).

At 0 °C under N₂, 3,5-bis(trifluoromethyl)phenyl isocyanate (0.149 g, 0.58 mmol, 0.1 mL) was added to a solution of 1-(2-(dimethylamino)naphthalen-yl)naphthalen-2-amine (0.158 g, 0.53 mmol) in 9 mL of dried CH₂Cl₂. The reaction mixture was stirred overnight at room temperature. After the evaporation of the solvent under *vacuum*, the remaining residue was purified using flash chromatography on silica gel (AcOEt/hexane = 1/10) affording the product as a yellow powder (86% yield, 0.260 g, 0.46 mmol). [α]_D = +163.1 (c 1.0, CHCl₃); ¹H NMR (CDCl₃, 400 MHz): δ = 8.07 (d, J = 8.0 Hz, 1H, ArH), 8.00 (d, J = 8.0 Hz, 1H, ArH), 7.93 (d, J = 8.0 Hz, 1H, ArH), 7.90 (d, J = 8.0 Hz, 1H, ArH), 7.79 (d, J = 8.0 Hz, 1H, ArH), 7.71 (s, 1H, NH), 7.47–7.43 (m, 3H, ArH), 7.37–7.16 (m, 5H, ArH), 7.13 (t, 1H, J = 8 Hz), 6.90 (d, 1H, J = 7.5 Hz), 6.63 (s, 1H, NH), 2.59 (s, 6H); ¹³C NMR (400 MHz, CDCl₃) δ : 152.6, 140.0, 133.5, 132.3, 131.8, 131.5, 130.2, 129.4, 128.3, 128.1, 126.9, 126.3, 125.4, 125.2, 124.8, 122.9, 118.7, 116.1, 43.8; anal. calcd. for C₃₁H₂₃N₃O F₆: C 65.61, H 4.08, N 7.40; found C 65.53, H 4.18, N 7.47.

2.2. General Procedure for the Enantioselective Organocatalyzed Vinylogous Addition of TMSOF to Benzaldehyde

A mixture of the catalyst (0.05 mmol) and the aldehyde (2.5 mmol) was stirred for 30 min at room temperature. Then, the TMSOF (84 μ L, 0.5 mmol) was slowly added for a period of 10 min, and the reaction mixture was stirred for 24 h at this temperature. The reaction progress was monitored by TLC (9.5/0.5 *v/v* CHCl₃/CH₃OH). At the end of the reaction, the mixture was cooled at –30 °C, and then treated with TFA. After 1h, the solution was quenched by adding a saturated aqueous NaHCO₃ solution, and the whole was stirred at room temperature for 10 min. The organic layer was separated, and the aqueous layer was repeatedly extracted with AcOEt (4 \times 10 mL). The combined organic extracts were dried (Na₂SO₄) and filtered. The filtrate was concentrated in *vacuo* and the residue was purified by chromatography (silica gel, CHCl₃) to give a mixture of the corresponding diastereomeric δ -hydroxymethylbutenolides. The diastereomeric ratio was determined by ¹H-NMR (400 MHz) analysis.

The enantiomeric excesses of the products were measured by chiral HPLC analyses (CHIRALPAK AD column with hexane/2-propanol 90/10, flow rate 0.8 mL/min: *Erythro* t_{R1} = 14.6 min, t_{R2} = 16.7 min; *Threo* t_{R1} = 19.3 min, t_{R2} = 20.3 min), in full analogy with the literature data [30].

3. Results and Discussion

3.1. Mono(thio)urea Catalysts **2** and **3**

The chiral thiourea derivative **2** was developed and utilized by Wang [32,33] for the organocatalysis of a Morita–Baylis–Hillman reaction and a nitro-Michael addition [32,33]. We envisioned that the chiral catalyst **2** could promote the enantioselective aldol addition reaction of TMSOF to aldehydes through asymmetric hydrogen-bonding activation. Thus, catalyst **2** was synthesized according to a procedure reported by Wang [32,33] and employed for the reaction between benzaldehyde **5** and TMSOF **4**. The reaction was carried out at room temperature with 0.5 mmol of TMSOF **4** and 2.5 mmol of benzaldehyde **5** using 10% of (*R,R*)-**2** under solvent-free conditions as reported in Figure 1b for organocatalyst **1** (Table 1).

As reported in Table 1 (entry 1), the reaction proceeded with a good diastereoselectivity (70/30 erythro/threo ratio), while showing a low catalytic activity (29% yield) and enantioselectivity (9% and 21% e.e.). At this point, we decided to explore the catalytic activity of the urea-based catalyst **3**. Therefore, urea derivative **3** was synthesized in good yield (86%)

with a procedure similar to that reported for **2** (see experimental section). Interestingly, under identical conditions, urea organocatalyst **3** shows an activity two times higher than the corresponding thiourea **2** (56% vs. 29% yield, respectively) with a concomitant slight improvement in enantioselectivity.

We conducted a computational study [36] on the conformational preferences of both organocatalysts, on their complexes with benzaldehyde, and on their H-bonding abilities to gain insights into this activity difference. We started our study considering all possible configurations around the ureido and thioureido functional group $R_1\text{-HN-C(X)-NH-R}_2$ ($X = \text{S/O}$) of free **2** and **3** (Figure 2), whose R_1 and R_2 substituents can be either *cis*- or *trans*-spatially oriented, to give a total of four different rotamers each (Figure 2).

A comprehensive DFT investigation at the B3LYP/6-31G(d,p) level of theory [37] on all four rotamers (Figure 2) of organocatalysts **2** and **3** showed that conformations **2-trans-A** and **3-trans-A** (Figures 2 and 3), both with *trans*-oriented R_1 and R_2 substituents, were the most stable ones (Table 2).

The **2-trans-A** conformation of organocatalyst **2** showed an intramolecular H-bonding interaction between the thioureido H atom and the nitrogen atom of the close dimethylamino $\text{N}(\text{CH}_3)_2$ substituent ($\text{HN}\cdots\text{N}$ distance of 2.94 Å and $\text{N-H}\cdots\text{N}$ angle of 139.7°) (Figure 3a). This intramolecular H-bonding interaction was lost in the **2-cis-A** rotamer which is less stable than its **2-trans-A** rotamer by 2.1 kcal/mol (Table 2). Analogously, this stabilizing intramolecular H-bonding interaction was also detected in the DFT-optimized structure of the **3-trans-A** rotamer, with a longer $\text{HN}\cdots\text{N}(\text{CH}_3)_2$ distance of 2.98 Å ($\text{N-H}\cdots\text{N}$ angle of 138.3°) (Figure 3b), which was lost in the **3-cis-A** rotamer. Interestingly, in this case, the ΔE (**3-trans-A**–**3-cis-A**) is reduced to 0.7 kcal/mol due to the weaker intramolecular $\text{N-H}\cdots\text{N}(\text{CH}_3)_2$ interaction, because of the lower acidity of the ureidic H atoms with respect to thioureido groups [38].

With these results in hand, we focused our attention on **5@2** and **5@3** supramolecular complexes with the catalysts in **2-trans-A**/**2-cis-A** and **3-trans-A**/**3-cis-A** conformations. In detail, the structure of the complexes was optimized by DFT calculations (see Supplementary Materials) and the secondary interactions stabilizing them were investigated by Non-Covalent Interaction (NCI) and Second-Order Perturbation Theory (SOPT) analysis of the Fock matrix in the Natural Bond Orbital (NBO) [39].

Concerning the supramolecular *cis/trans* complexes **5@2**, the **5@2-trans-A** rotamer is more stable (Figure 4a) than **5@2-cis-A**, with an energy difference of 1.5 kcal/mol. Close inspection of the DFT-optimized structure of **5@2-trans-A** revealed, also in this case, the presence of a stabilizing intramolecular H-bonding interaction $\text{NHC(S)N-H}\cdots\text{N}(\text{CH}_3)_2$ ($\text{HN}\cdots\text{N}$ distance of 2.94 Å and $\text{N-H}\cdots\text{N}$ angle of 139.6°) (Figure 4a).

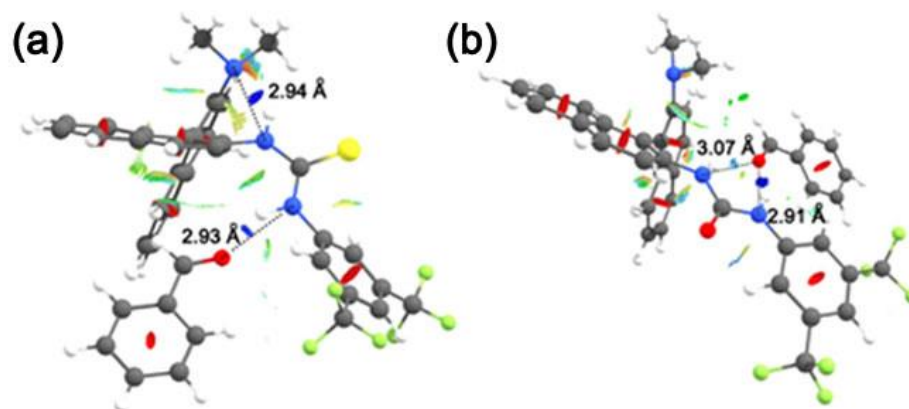


Figure 4. Non-Covalent Interaction plots by the sign of the second Hessian eigenvalue (gradient isosurfaces ($s = 0.5$ a.u.) of complex **5@2-trans-A** (a) and **5@3-cis-A** (b).

Differently, for the complexes of catalyst **3**, the relative stabilities of the two *cis/trans* rotamers were inverted. In fact, the **5@3-cis-A** rotamer is more stable by 1.4 kcal/mol with

respect to **5@3-trans-A** (Table 2). In this case, the intramolecular NHC(O)N–H...N(CH₃)₂ H bond is lost, while two intermolecular H bonds between the ureido group of **3-cis-A** and the carbonyl of **5** (HN...O distances of 2.91 and 3.07 Å) are present (Figure 4b).

NBO and NCI calculations for the complex **5@2-trans-A** (Figure 4a) show the presence of a H-bonding interaction between the carbonyl group of benzaldehyde **5** and the thioureido NH group of **2**, through LP(2) → σ* donation between the oxygen atom of **5** and a N–H antibonding orbital of **2**. A N...O distance of 2.93 Å and a N–H...O angle of 147.0° were measured and this H-bonding interaction accounts for 83% of the total interaction energy (TIE).

An interesting result was obtained for the **5@3-cis-A** complex, where two H-bonding interactions were computed between N–H atoms of the urea group and the oxygen atom of **5** (HN...O distances 3.07 Å and 2.91 Å, N–H...O angles of 149.9° and 160.7°) which account for 89% of TIE. In addition, a weak van der Waals interaction was also computed between the *ortho* aromatic H atom of **5** and the 3,5-trifluoromethyl group, which accounts for 5% of TIE.

DFT calculations (see experimental section) indicated that the *cis* complexes showed coordination energies [34] of 5.4 and 7.8 kcal/mol, respectively, for **5@2-cis-A** and **5@3-cis-A**, and the *trans* complexes of 4.7 and 5.7 kcal/mol, respectively, for **5@2-trans-A** and **5@3-trans-A** (see data in Table 2). In summary, these data strongly indicated that for both catalysts **2** and **3**, the *cis* rotamers show stronger H-bonding interactions with the aldehyde substrate **5**, as a consequence of the double intermolecular H bond formation. Consequently, for an efficient activation of **5**, a *cis* conformation of the HN–CX–NH unit is needed. Thus, a conformational *trans-A* → *cis-A* interconversion is necessary for both catalysts **2** and **3** before aldehyde **5** coordination. Based on ΔE (*cis-trans*) values of 2.1 and 0.7 kcal/mol calculated for free rotamers of the catalysts **2** and **3**, Boltzmann distributions of 3/97 and 24/76 were calculated for their *cis/trans* rotamers, respectively. Consequently, the higher percentage of *cis*-rotamer of **3** and its higher coordination energy in **5@3-cis-A** (7.8 kcal/mol) justify its higher catalytic efficiency (56% yield) with respect to catalyst **2** (coordination energy in **5@2-cis-A** of 5.4 kcal/mol; 29% yield).

3.2. Bis(thio)urea Catalysts **7** and **8**

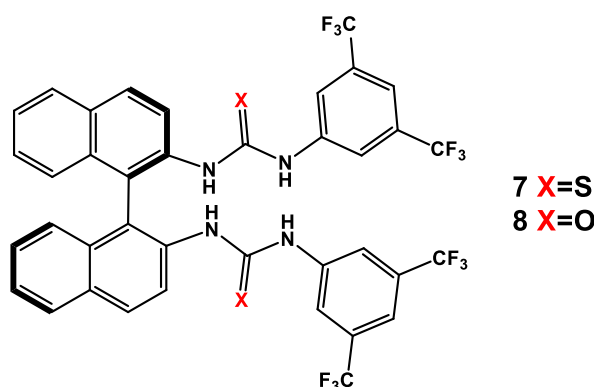
To increase the enantioselectivity of the reaction, we decided to test the catalytic activity of chiral bis(thio)urea derivatives **7** and **8** (Table 3) that possess a stronger H-bonding ability. Bis(thio)ureas were used as chiral fluorescent receptors for anions [40] but also as efficient catalysts for the asymmetric MBH reaction [41,42]. These structurally diverse potential catalysts are easily accessible by the condensation of chiral BINAM diamine with two equivalents of iso(thio)cyanate [34]. Therefore, derivatives **7** and **8** were synthesized according to reported procedures [34] and then screened in the model reaction of benzaldehyde **5** with TMSOF **4**. The results are reported in Table 3.

When bis-thiourea **7** was used (entry 1, Table 3) as the catalyst, a greater catalytic efficiency (45% yield) was observed with respect to the mono-thiourea **2**; in addition, the enantioselectivity of *threo-6* isomer was improved from 21% to 93%, while in the case of the *erythro-6*, from 9% to 32%. Very surprisingly, in the presence of **7**, the diastereomeric *erythro/threo* ratio of the products was totally inverted in favor of the *threo* isomer (passing from 70/30 to 30/70). A slight improvement in the yield (from 45% to 53%) was observed in going from bis-thiourea **7** to bis-urea **8** (entry 2, Table 3), in spite of the greater acidity of the thioureidic hydrogens over the ureidic ones [38]. An increase in the reaction time (entries 3–6) had little effect on the chemical yield and the diastereoisomeric ratio, but the enantioselectivity of both *erythro*- and *threo-6* isomers was progressively lowered.

In order to optimize the reaction conditions and to determine the number of catalytically active sites of bis-urea catalyst **8**, we evaluated the dependence of the reaction efficiency on the concentration of reagents (Table 4). The experiments revealed that the catalytic activity of **8** strongly depends on the benzaldehyde concentration in the reaction environment; when the reaction was carried out by using a lower amount of benzalde-

hyde **5** (from 5 to 3 mmol), the chemical yield was increased (from 53% to 70%, entries 1–2, Table 4), but the diastereo- and enantioselectivity of the *erythro* and *threo* isomers were lowered. As the diene/aldehyde ratio was increased from 1:5 to 1:1 (entry 3, Table 4), no significant difference in efficiency was observed but, unfortunately, a loss of diastereo- and enantio-selectivity took place. With the aim to verify if the benzaldehyde excess (liquid compound) only served to prevent the self-assembly of the catalyst, we performed the reaction in toluene solvent by maintaining constant the concentration of the catalyst in solution (entry 4, Table 4); the yield was higher, but both the diastereoselectivity and enantioselectivity were scarce. The same trend was observed for the reactions with three and five equivalents of diene (entries 5–6, Table 4): low diastereoselectivity and low selectivity were observed in both instances.

Table 3. Addition reaction of TMSOF **4** to benzaldehyde **5** catalyzed by bis(thio)urea catalysts **7** and **8**¹.



Entry	Catalyst	Equivalents of Aldehyde	T/t (°C/h)	Yield (%) ²	d.r. Erythro/Threo ³	e.e. ⁴ Erythro (%)	e.e. ⁴ Threo (%)
1	7	5	Rt/24	45	30/70	32	93
2	8	5	Rt/24	53	30/70	45	90
3	7	5	Rt/48	45	30/70	20	91
4	8	5	Rt/48	53	37/63	39	89
5	7	5	Rt/72	50	30/70	15	91
6	8	5	Rt/72	45	34/66	36	85

¹ The reactions were performed with 0.5 mmol of TMSOF and 10 mol% catalyst was used. ² Isolated yield. ³ The diastereoisomeric ratio was calculated by ¹H NMR of the crude product according to the literature data [43]. ⁴ The e.e. values were determined by chiral HPLC analysis.

Table 4. Vinylogous aldol reaction catalyzed by bis-urea catalyst **8**¹.

Entry	TMSOF/Aldehyde	T/t (°C/h)	Solvent	Yield (%) ²	d.r. (Erythro/Threo) ³	e.e. (%) Erythro ⁴	e.e. (%) Threo ⁴
1	1/5	Rt/24	-	53	30/70	45	90
2	1/3	Rt/24	-	70	44/56	36	84
3	1/1	Rt/24	-	45	50/50	6	62
4	1/1	Rt/24	Toluene (0.2 mL)	62	48/52	2	24
5	3/1	Rt/24	-	43	67/33	26	46
6	5/1	Rt/24	-	51	57/43	16	28

¹ The reactions were performed with 0.5 mmol of TMSOF and 10 mol% catalyst was used. ² Isolated yield. ³ The diastereoisomeric ratio was calculated by ¹H NMR of the crude product according to the literature data [43]. ⁴ The e.e. values were determined by chiral HPLC analysis.

These results clearly indicated that the selectivity of the reaction was related to the ratio of diene to aldehyde, and they showed that, under the same reaction conditions, increasing the concentration of aldehyde in the reaction environment increased the d.r. in

favor of the syn-isomer (*threo*) while an increase in diene determined a prevalence of the anti-isomer (*erythro*) (Figure 5a).

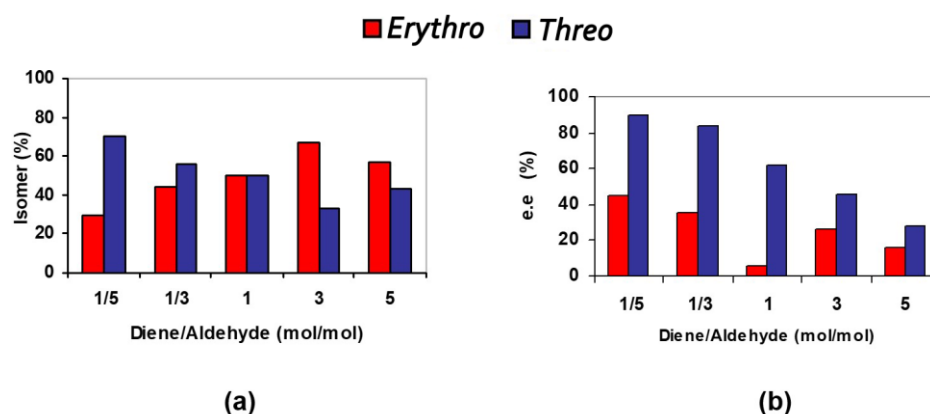


Figure 5. (a) Diastereoisomeric distribution (%) versus diene/aldehyde molar ratio. (b) Enantiomeric excess versus diene/aldehyde molar ratio.

The *ee*'s of both isomers also show a strong dependence on the aldehyde concentration (Figure 5b): an increase in the amount of diene determines a linear lowering of the enantiomeric excess of the *threo* isomer and a progressive increase in the enantiomeric excess of the *erythro* isomer.

To identify the possible active sites of bis-(thio)urea catalysts **7** and **8**, a conformational analysis was performed (Figure 6 and Table 2). The three most stable rotamers, among all the possible ones, were obtained by conformational searching for the free organocatalysts **7** and **8**: *cis-cis*, *cis-trans*, and *trans-trans*. The optimized structures were obtained by DFT calculations at the B3LYP/6-31G(d,p) level of theory [38] and are reported in Figure 6 (the corresponding energies are reported in Table 2).

As concerns bis-thiourea **7**, its *trans-trans* conformation is the most stable (Figure 6c, left, Table 2), whereas for bis-urea **8** the greatest stability was found for the *cis-cis* conformation (Figure 6a, right, Table 5).

Table 5. Relative stabilities between rotamers of Figure 6 and coordination energies for the formation of 5@8-*cis-cis* and (5)₂@8-*cis-cis* complexes.

Rotamers	$\Delta E_{\text{isomer}}^1$ (kcal/mol)	E_{coord} (kcal/mol)
7- <i>cis-cis</i>	1.77	-
7- <i>trans-cis</i>	2.41	-
7- <i>trans-trans</i>	0.00	-
8- <i>cis-cis</i>	0.00	-
8- <i>trans-cis</i>	5.33	-
8- <i>trans-trans</i>	8.07	-
5@8- <i>cis-cis</i>	-	-8.9
(5) ₂ @8- <i>cis-cis</i>	-	-12.9

¹ ΔE_{isomer} is calculated assuming the energy of the most stable conformer as zero.

In fact, as highlighted in Figure 6a, organocatalyst **8** preferentially adopts the *cis-cis* conformation stabilized by intramolecular N-H...O=C H-bonding interactions between both ureido groups, which are absent in catalyst **7** bearing thiourea groups. Concerning catalyst **7**, the most stable conformation is *trans-trans* (Table 5), in agreement with the data previously reported in the literature for this derivative [37]. Insights on the intramolecular secondary interactions that stabilize the *trans-trans* conformation of **7** were obtained by DFT calculations and NBO and NCI studies. The results highlight the presence of weak

H-bonding *Aromatic*C–H...S=C interactions through LP(S) → C–H antibonding σ^* orbital donation (Figure 7), between an aromatic hydrogen atom of BINAM and S=C thioureido group (C–H...S=C distance of 2.86 Å, and C–H...S angle of 104.9°, see Supplementary Materials). In the literature, these interactions were recently compared to weak H-bonding interactions [44], and in this case, they account for 3.6 kcal·mol^{−1} of TIE. In addition, π – π interactions between aromatic rings of BINAM and 3,5-bis(trifluoromethyl)-phenyl groups were detected (see Supplementary Materials).

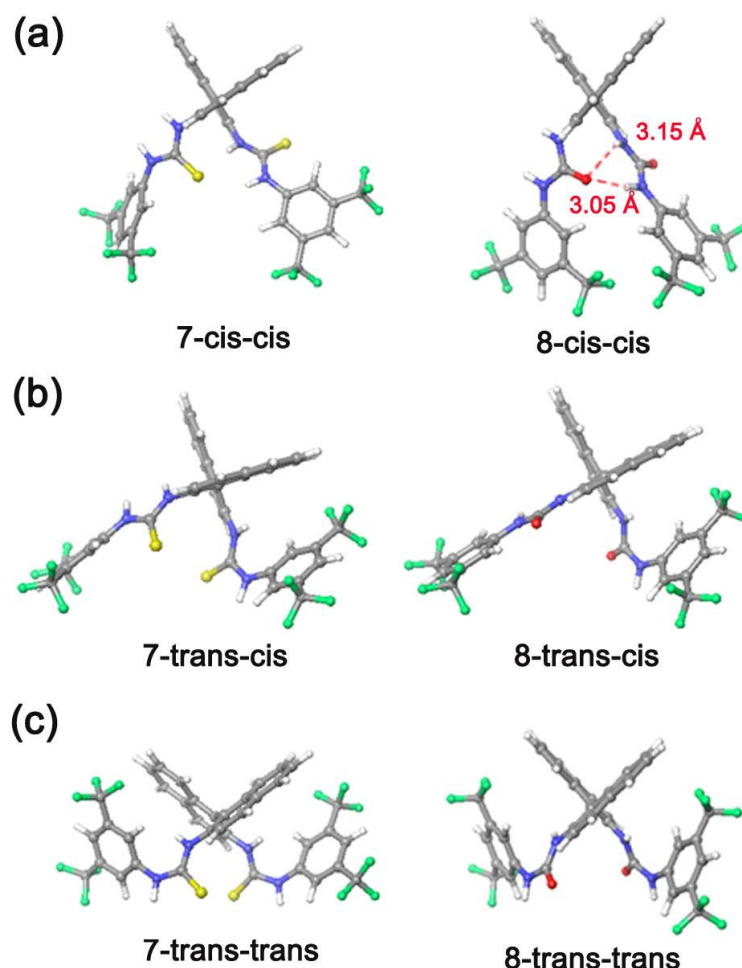


Figure 6. DFT-optimized structures for: (a) cis-cis rotamers of catalysts 7 (left side) and 8 (right side); (b) trans-cis rotamers of catalysts 7 (left side) and 8 (right side); (c) trans-trans rotamers of catalysts 7 (left side) and 8 (right side).

Based on such information, the active site analysis was carried out for the *cis-cis* conformation of catalyst 8 (Figure 6). The structures of the complexes $5@8$ -*cis-cis* (Figure 8b) and $(5)_2@8$ -*cis-cis* (Figure 8c) were optimized by DFT calculations, and the secondary interactions between aldehyde 5 and catalyst 8 were investigated using the Non-Covalent Interaction (NCI) and Second-Order Perturbation Theory (SOPT) analysis of the Fock matrix in the Natural Bond Orbital (NBO) [39].

For this conformation, it is possible to hypothesize two different coordination (or activation) sites: an “open site” (Figure 8a), with ureidic NH groups pointing toward the exterior of the molecule, and a “pocket site”, with NHs pointing toward the molecular interior. Figure 8 displays the DFT-optimized structure of the complexes $5@8$ -*cis-cis* (Figure 8b) and $(5)_2@8$ -*cis-cis* (Figure 8c).

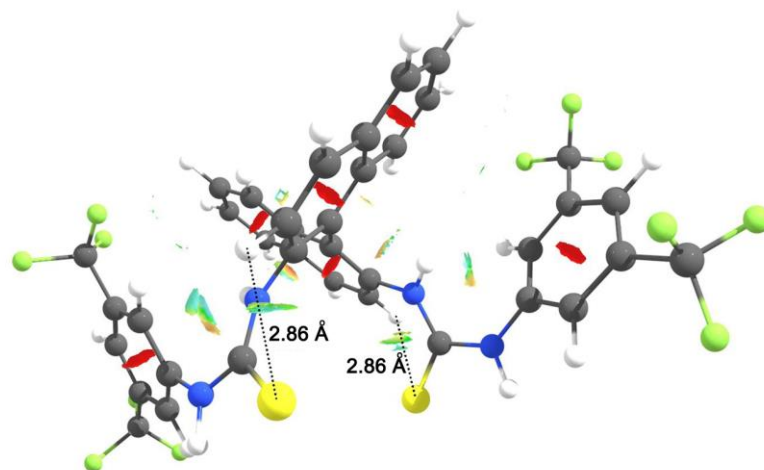


Figure 7. Non-Covalent Interaction plots by the sign of the second Hessian eigenvalue (gradient isosurfaces $s = 0.5$ a.u.) of 7-*trans-trans*. Marked the C-H...S=C distances in weak C-H...S=C H-bonding interactions [37].

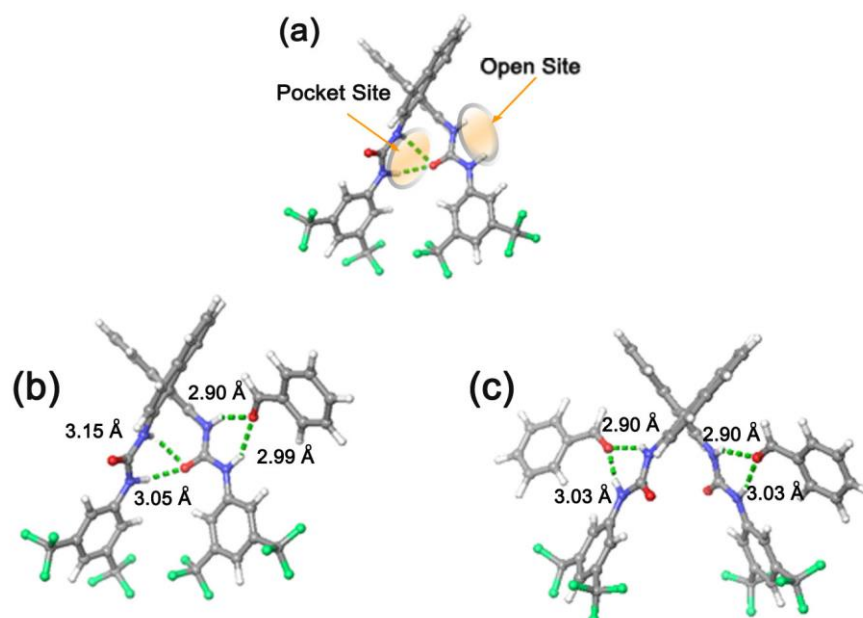


Figure 8. (a) Schematic view of the two possible aldehyde activation sites for organocatalyst 8. DFT-optimized structures of complexes 5@8-*cis-cis* (b) and (5)₂@8-*cis-cis* (c).

The optimized structure of the 1:1 complex 5@8-*cis-cis* (Figure 8b) shows intramolecular H bonds between the urea NHs of the pocket site and the C=O of the close urea group of the open site. In addition, two intermolecular H-bonding interactions were detected (N...O distances 2.90 Å and 2.99 Å and N-H...O angles of 155.2° and 151.3°) between the C=O of benzaldehyde 5 and the NHs of the open site. NBO studies reveal LP(2) → σ* donations between the oxygen atom of 5 and a N-H antibonding orbital of 8 which account for 92% of TIE.

Regarding the (5)₂@8-*cis-cis* complex, four intermolecular H-bonding interactions were computed between two molecules of aldehyde 5 and ureidic NH groups of 8 (Figure 8c). NBO studies (Figure 9) highlighted LP(2) → σ* donations between the oxygen atom of aldehyde 5 to a N-H antibonding orbital of 8, which account for 92% of TIE. Finally, CH...π interactions were detected between the aldehydic hydrogen atom of 5 and the aromatic rings of 8 (see Figure 9, center) which play a role in the stabilization of the (5)₂@8-*cis-cis* complex (6% of TIE).

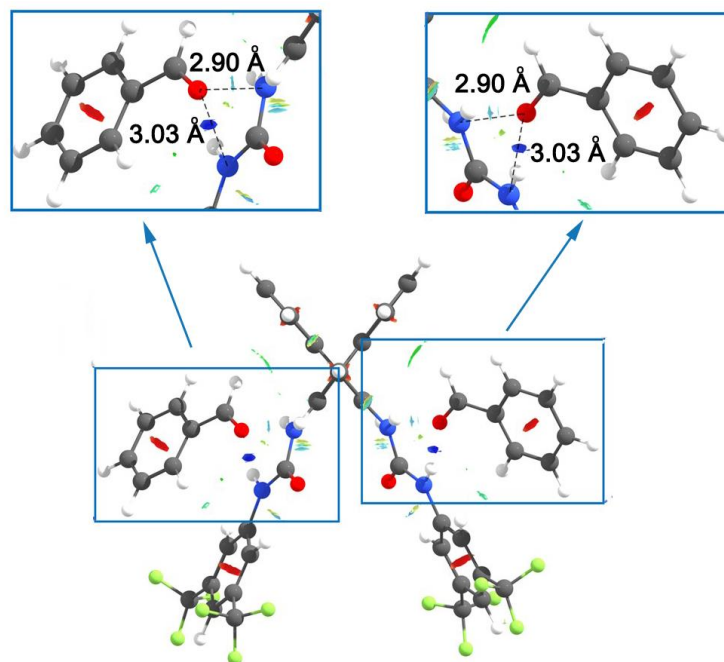


Figure 9. Non-Covalent Interaction plots by the sign of the second Hessian eigenvalue (gradient isosurfaces ($s = 0.5$ a.u.) for the 1:2 optimized complex of **8** with two molecules benzaldehyde **5**. Details of the H-bonding interactions are in the insets.

Also, in this case, the coordination energies (see Supplementary Materials) were calculated for the DFT-optimized structures of $5@8$ -*cis-cis* and $(5)_2@8$ -*cis-cis* complexes and by their corresponding single-point energies (see experimental section). Starting with the DFT-optimized structure of the catalyst **8**-*cis-cis* in Figure 8a, the complexation of a benzaldehyde molecule **5** in the open site of **8** (Figure 8b), in accordance with the process $5 + 8$ -*cis-cis* = $5@8$ -*cis-cis*, accounts for a coordination energy of -8.9 kcal/mol (see Table 4); meanwhile, the complexation of a second molecule of **5** in the pocket site of the $5@8$ -*cis-cis* complex in Figure 8b ($5 + 5@8$ -*cis-cis* = $(5)_2@8$ -*cis-cis*) (see Figure 8c) accounts for an extra stabilization of -4.0 kcal/mol (total coordination energy of the $(5)_2@8$ -*cis-cis* complex, -12.9 kcal/mol, see Table 4).

These results strongly suggest that the coordination of a second benzaldehyde molecule in the pocket site of the $5@8$ -*cis-cis* complex to form the $(5)_2@8$ -*cis-cis* complex is significantly less favored than the first coordination at the open site to give $5@8$ -*cis-cis*. Of course, this is due to the loss of two intramolecular hydrogen bonds between the urea groups incorporated in the open and pocket sites of the $5@8$ -*cis-cis* complex, upon coordination of the second aldehyde **5**.

From these results, we can conclude that the two coordination (activation) sites show, in principle, the same possibility to activate an aldehyde molecule, particularly when an excess of **5** is used (1/3 or 1/5, see Table 3). When a lower amount of aldehyde **5** is used (i.e., entry 2, Table 3) it is likely that a high percentage of the open site is singly occupied. This could lead to a higher catalytic activity (70% yield) because of the presence of cooperative intramolecular H-bonding interactions by the urea NHs of the pocket site. Under such conditions, the maximum enantioselectivity (*erythro* 45% *e.e.*; *threo* 90% *e.e.*) is observed (entry 1, Table 3) probably due to a double occupancy of two stereochemically equivalent sites.

4. Conclusions

In summary, we have described a highly efficient organocatalytic method for the enantioselective vinylogous addition reaction of the TMSOF to benzaldehyde. High levels of diastereoselectivity and enantioselectivity have been achieved by using easily prepared (thio)urea derivatives. In accordance with previous reports, the above results suggest a catalytic mechanism in which the aldehyde is activated upon coordination with a (thio)ureidic compound. It has been found that, despite the higher acidity of thioureidic derivatives, ureidic derivatives can be conveniently used as efficient catalysts in this aldol reaction. Moreover, the structure and the energetic features of the organocatalysts and their complexes with benzaldehyde were investigated by DFT calculations. The main obtained conclusions are the following: (1) For an efficient activation of the substrate, a double H bond formation is needed. The stronger tendency of catalyst **2**, with respect to **3**, to present a *trans* conformation of the two H atoms of the HN-CS-NH unit can explain the lower activity of this system. (2) For systems **7** and **8**, an active site model was proposed to explain the high reaction selectivity. Finally, the simplicity of the experimental procedure and the ready accessibility of the catalysts give a powerful method for constructing chiral δ -substituted γ -hydroxymethyl-butenolides.

Supplementary Materials: The following supporting information can be downloaded at <https://www.mdpi.com/article/10.3390/org5020003/s1>, Computational Details, Atomic Coordinates, and NCI Studies Details.

Author Contributions: Conceptualization, A.S. and P.N.; methodology, V.I.; data curation, P.D.S.; writing—original draft preparation, M.D.R.; writing—review and editing, C.G.; visualization, C.T. All authors have read and agreed to the published version of the manuscript.

Funding: This research was funded by the UNIVERSITY of SALERNO, FARB 2021.

Data Availability Statement: All data for this work are included in the manuscript and the Supplementary Materials.

Conflicts of Interest: The authors declare no conflicts of interest.

References

1. Breslow, R. Artificial Enzymes. *Science* **1982**, *218*, 532–537. [[CrossRef](#)]
2. McMillan, D.W.C. The advent and development of organocatalysis. The advent and development of organocatalysis. *Nature* **2008**, *455*, 304–308. [[CrossRef](#)] [[PubMed](#)]
3. Raynal, M.; Ballester, P.; Vidal-Ferran, A.; van Leeuwen, P.W.N.M. Supramolecular catalysis. Part 1: Non-covalent interactions as a tool for building and modifying homogeneous catalysts. *Chem. Soc. Rev.* **2014**, *43*, 1660–1733. [[CrossRef](#)]
4. Purse, B.W.; Rebek, J., Jr. Functional cavitands: Chemical reactivity in structured environments. *Proc. Natl. Acad. Sci. USA* **2005**, *102*, 10777–10782. [[CrossRef](#)]
5. Meeuwissen, J.; Reek, J.N.H. Supramolecular catalysis beyond enzyme mimics. *Nat. Chem.* **2010**, *2*, 615–621. [[CrossRef](#)] [[PubMed](#)]
6. Gambaro, S.; Talotta, C.; Della Sala, P.; Soriente, A.; De Rosa, M.; Gaeta, C.; Neri, P.J. Kinetic and Thermodynamic Modulation of Dynamic Imine Libraries Driven by the Hexameric Resorcinarene Capsule. *Am. Chem. Soc.* **2020**, *142*, 14914–14923. [[CrossRef](#)] [[PubMed](#)]
7. Lloyd, G.; Forgan, R.S. (Eds.) Reactivity in Confined Spaces. In *Monographs in Supramolecular Chemistry*; The Royal Society of Chemistry: London, UK, 2021.
8. Iuliano, V.; Della Sala, P.; Talotta, C.; De Rosa, M.; Soriente, A.; Gaeta, C.; Neri, P. Supramolecular control on reactivity and selectivity inside the confined space of H-bonded hexameric capsules. *Curr. Opin. Colloid Interface* **2023**, *65*, 101692. [[CrossRef](#)]
9. Borsato, G.; Rebek, J., Jr.; Scarso, A. *From Selective Nanocatalysts and Nanoscience*; Zecchina, A., Bordiga, S., Groppo, E.E., Eds.; Wiley-VCH Verlag GmbH & Co. KGaA: Weinheim, Germany, 2011; pp. 105–168.
10. Catti, L.; Zhang, Q.; Tiefenbacher, K. Advantages of Catalysis in Self-Assembled Molecular Capsules. *Chem. Eur. J.* **2016**, *22*, 9060–9066. [[CrossRef](#)]
11. Hong, C.M.; Bergman, R.G.; Raymond, K.N.; Toste, F.D. Self-Assembled Tetrahedral Hosts as Supramolecular Catalysts. *Acc. Chem. Res.* **2018**, *51*, 2447–2455. [[CrossRef](#)]
12. Ren, Y.; Tao, L.; Li, C.; Jayakumar, S.; Li, H.; Yang, Q. Development of Efficient Solid Chiral Catalysts with Designable Linkage for Asymmetric Transfer Hydrogenation of Quinoline Derivatives. *Chin. J. Catal.* **2021**, *42*, 1576–1585. [[CrossRef](#)]
13. Wang, B.; Jin, C.; Shao, S.; Yue, Y.; Zhang, Y.; Wang, S.; Chang, R.; Zhang, H.; Zhao, J.; Li, X. Electron-Deficient Cu Site Catalyzed Acetylene Hydrochlorination. *Green Energy Environ.* **2023**, *8*, 1128–1140. [[CrossRef](#)]

14. Zhang, Z.; Zhang, H.; Wang, B.; Yue, Y.; Zhao, J. Migration: A Neglected Potential Contribution of HCl-Oxidized Au(0). *Molecules* **2023**, *28*, 1600. [[CrossRef](#)]
15. Doyle, A.G.; Jacobsen, E.N. Small-Molecule H-Bond Donors in Asymmetric Catalysis. *Chem. Rev.* **2007**, *12*, 5713–5743. [[CrossRef](#)]
16. Taylor, M.S.; Jacobsen, E.N. Asymmetric Catalysis by Chiral Hydrogen-Bond Donors. *Angew. Chem. Int. Ed.* **2006**, *45*, 1520–1543. [[CrossRef](#)]
17. Li, S.; Du, J.; Zhang, B.; Liu, Y.; Mei, Q.; Meng, Q.; Dong, M.; Du, J.; Zhao, Z.; Zheng, L.; et al. Selective Hydrogenation of 5-(Hydroxymethyl)Furfural to 5-Methylfurfural by Exploiting the Synergy between Steric Hindrance and Hydrogen Spillover. *Acta Phys. Chim. Sin.* **2022**, *38*, 2206019. [[CrossRef](#)]
18. Wang, K.; Wang, B.; Liu, X.; Fan, H.; Liu, Y.; Li, C. Palladium-Catalyzed Enantioselective Linear Allylic Alkylation of Vinyl Benzoxazinones: An Inner-Sphere Mechanism. *Chin. J. Catal.* **2021**, *42*, 1227–1237. [[CrossRef](#)]
19. Cafeo, G.; De Rosa, M.; Kohnke, F.H.; Neri, P.; Soriente, A.; Valenti, L. Efficient organocatalysis with a calix[4]pyrrole derivative. *Tetrahedron Lett.* **2008**, *49*, 153–155. [[CrossRef](#)]
20. Cafeo, G.; De Rosa, M.; Kohnke, F.H.; Soriente, A.; Talotta, C.; Valenti, L. Calixpyrrole Derivatives: “Multi Hydrogen Bond” Catalysts for γ -Butenolide Synthesis. *Molecules* **2009**, *14*, 2594–2601. [[CrossRef](#)]
21. De Rosa, M.; Citro, L.; Soriente, A. The first organocatalytic addition of 2-trimethylsilyloxyfuran to carbonyl compounds: Hydrogen-bond catalysis in γ -butenolides synthesis. *Tetrahedron Lett.* **2006**, *47*, 8507–8510. [[CrossRef](#)]
22. Smith, C.J.; Abbanat, D.; Bernan, V.S.; Maiese, W.M.; Greenstein, M.; Jompa, J.; Tahir, A.; Ireland, C.M.J. Novel Polyketide Metabolites from a Species of Marine Fungi. *Nat. Prod.* **2000**, *63*, 142–145. [[CrossRef](#)]
23. Antane, S.; Caufield, C.E.; Hu, W.; Keeney, D.; Labthavikul, P.; Morris, K.; Naughton, S.M.; Petersen, P.J.; Rasmussen, B.A.; Singh, G.; et al. Pulvinones as bacterial cell wall biosynthesis inhibitors. *Bioorg. Med. Chem. Lett.* **2006**, *16*, 176–180. [[CrossRef](#)]
24. Li, R.-T.; Han, Q.-B.; Zheng, Y.-T.; Wang, R.-R.; Yang, L.-M.; Lu, Y.; Sang, S.-Q.; Zheng, Q.-T.; Zhao, Q.-S.; Sun, H.-D. Structure and anti-HIV activity of micrandilactones B and C, new norriterpenoids possessing a unique skeleton from *Schisandra micrantha*. *Chem. Commun.* **2005**, *23*, 2936–2938. [[CrossRef](#)]
25. Yu, C.; Ji, P.; Zhang, Y.; Meng, X.; Wang, W. Construction of Enantioenriched γ,γ -Disubstituted Butenolides Enabled by Chiral Amine and Lewis Acid Cascade Cocatalysis. *Org. Lett.* **2021**, *23*, 7656–7660. [[CrossRef](#)]
26. Hug, J.J.; Kjaerulf, L.; Garcia, R.; Müller, R. New Deoxyenhygrolides from *Plesiocystis pacifica* Provide Insights into Butenolide Core Biosynthesis. *Mar. Drugs* **2022**, *20*, 72. [[CrossRef](#)]
27. Pelter, A.; Al-Bayati, R.I.H.; Ayoub, M.T.; Lewis, W.; Pardasani, P.; Hänsel, R. Synthetic routes to the piperolides, fadyenolides, epoxy piperolides, and related compounds. *J. Chem. Soc. Perkin Trans.* **1987**, *1*, 717–742. [[CrossRef](#)]
28. Boukouvalas, J.; Maltais, F. An efficient total synthesis of the antibiotic patulin. *Tetrahedron Lett.* **1995**, *36*, 7175–7176. [[CrossRef](#)]
29. Brown, S.P.; Goodwin, N.C.; MacMillan, D.W.C.J. The First Enantioselective Organocatalytic Mukaiyama–Michael Reaction: A Direct Method for the Synthesis of Enantioenriched γ -Butenolide Architecture. *J. Am. Chem. Soc.* **2003**, *125*, 1192–1194. [[CrossRef](#)] [[PubMed](#)]
30. Singh, R.P.; Foxman, B.M.; Deng, L. Asymmetric Vinylogous Aldol Reaction of Silyloxy Furans with a Chiral Organic Salt. *J. Am. Chem. Soc.* **2010**, *132*, 9558–9560. [[CrossRef](#)] [[PubMed](#)]
31. Pansare, S.V.; Paul, E.K. The Organocatalytic Vinylogous Aldol Reaction: Recent Advances. *Chem. Eur. J.* **2011**, *17*, 8770–8779. [[CrossRef](#)] [[PubMed](#)]
32. Wang, J.; Li, H.; Yu, X.; Zu, L.; Wang, W. Chiral Binaphthyl-Derived Amine-Thiourea Organocatalyst-Promoted Asymmetric Morita–Baylis–Hillman Reaction. *Org. Lett.* **2005**, *7*, 4293–4296. [[CrossRef](#)]
33. Wang, J.; Li, H.; Duan, W.; Zu, L.; Wang, W. Organocatalytic Asymmetric Michael Addition of 2,4-Pentandione to Nitroolefins. *Org. Lett.* **2005**, *7*, 4713–4716. [[CrossRef](#)]
34. Fleming, E.M.; McCabe, T.; Connon, S.J. Novel axially chiral bis-arylthiourea-based organocatalysts for asymmetric Friedel–Crafts type reactions. *Tetrahedron Lett.* **2006**, *47*, 7037–7042. [[CrossRef](#)]
35. Ollevier, T.; Bouchard, J.-E.; Desyroy, V. Diastereoselective Mukaiyama Aldol Reaction of 2-(Trimethylsilyloxy)Furan Catalyzed by Bismuth Triflate. *J. Org. Chem.* **2008**, *73*, 331–334. [[CrossRef](#)]
36. Della Sala, P.; Del Regno, R.; Capobianco, A.; Iuliano, V.; Talotta, C.; Geremia, S.; Hickey, N.; Neri, P.; Gaeta, C. Confused-Prism[5]arene: A Conformationally Adaptive Host by Stereoselective Opening of the 1,4-Bridged Naphthalene Flap. *Chem. Eur. J.* **2023**, *29*, e2022030. [[CrossRef](#)]
37. Zhu, J.-L.; Zhang, Y.; Liu, C.; Zheng, A.-M.; Wang, W.J. Insights into the Dual Activation Mechanism Involving Bifunctional Cinchona Alkaloid Thiourea Organocatalysts: An NMR and DFT Study. *Org. Chem.* **2012**, *77*, 9813–9825. [[CrossRef](#)] [[PubMed](#)]
38. Jakab, G.; Tancon, C.; Zhang, Z.; Lippert, M.K.; Schreiner, P.R. (Thio)urea Organocatalyst Equilibrium Acidities in DMSO. *Org. Lett.* **2012**, *14*, 1724–1727. [[CrossRef](#)]
39. Weinhold, F.; Landis, C.R. *Valency and Bonding: A Natural Bond Orbital Donor-Acceptor Perspective*, 1st ed.; Cambridge University Press: Cambridge, UK, 2003.
40. Lan-Hua, W.; Yong-Bing, H.; Kuo-Xi, X.; Shun-Ying, L.; Ling-Zhi, M. Chiral Fluorescent Receptors Based on (R)-1,1'-Binaphthylene-2,2'-bis-thiourea: Synthesis and Chiral Recognition. *Chin. J. Chem.* **2005**, *23*, 757–761. [[CrossRef](#)]
41. Sohtome, Y.; Tanatani, A.; Hashimoto, Y.; Nagasawa, K. Development of bis-thiourea-type organocatalyst for asymmetric Baylis–Hillman reaction. *Tetrahedron Lett.* **2004**, *45*, 5589–5592. [[CrossRef](#)]

42. Berkessel, A.; Roland, K.; Neudörfl, J.M. Asymmetric Morita–Baylis–Hillman Reaction Catalyzed by Isophoronediamine-Derived Bis(thio)urea Organocatalysts. *Org. Lett.* **2006**, *8*, 4195–4198. [[CrossRef](#)]
43. Szlosek, M.; Figadère, B. Highly Enantioselective Aldol Reaction with 2-Trimethylsilyloxyfuran: The First Catalytic Asymmetric Autoinductive Aldol Reaction. *Angew. Chem. Int. Ed.* **2000**, *39*, 1799–1801. [[CrossRef](#)]
44. Ghosh, S.; Chopra, P.; Wategaonkar, S. C–H ··· S interaction exhibits all the characteristics of conventional hydrogen bonds. *Phys. Chem. Chem. Phys.* **2020**, *22*, 17482–17493. [[CrossRef](#)]

Disclaimer/Publisher’s Note: The statements, opinions and data contained in all publications are solely those of the individual author(s) and contributor(s) and not of MDPI and/or the editor(s). MDPI and/or the editor(s) disclaim responsibility for any injury to people or property resulting from any ideas, methods, instructions or products referred to in the content.